ELSEVIER

Biophysical Chemistry 125 (2007) 444–452

Biophysical Chemistry

http://www.elsevier.com/locate/biophyschem

In vitro investigation of the geometric contraction behavior of chemo-mechanical P-protein aggregates (forisomes)

S. Schwan, M. Fritzsche, A. Cismak, A. Heilmann, U. Spohn *

Fraunhofer Institute of Mechanics of the Materials, Heideallee 19, D-06120 Halle, Germany

Received 1 June 2006; received in revised form 13 October 2006; accepted 16 October 2006
Available online 26 October 2006

Abstract

We investigated the contracting behavior of forisomes from *Vicia faba* by carrying out precise measurements of their changing geometric parameters *in vitro* in the absence and in the presence of dissolved oxygen. Furthermore, we investigated the fine structure of forisomes by scanning electron microscopy. For the first time, single forisomes were titrated with Ca^{2+}, protons, and hydroxide ions recording the complete progression of their contractions. An apparent Ca^{2+}-binding constant of (22±3) μM was calculated from two complete titration curves. The forisomes also contracted in the presence of Ba^{2+} and Sr^{2+} ions, but the amplitudes of contraction were smaller under the same measuring conditions. The time taken to change from the longitudinally expanded into the longitudinally contracted state was up to 2 s shorter in 10 mM Ca^{2+} in comparison to 0.2 mM Ca^{2+}. However, the contraction time was prolonged by decreasing the Ca^{2+} concentration. In the absence of dissolved oxygen, the transition between the two final states of the forisomes was almost reversible and the amplitude of contraction remained almost constant during the first 25 contraction cycles. In the presence of dissolved oxygen the forisomes denaturated after a few cycles and lost their ability to contract, just after only a few cycles with 10 min in the contracted state. Denaturation of the forisomes occurred appreciably in the contracted state. We propose a cycle process to explain the thermodynamic basis of the Ca^{2+}-induced contraction and its reversal by EDTA. Reducing the pH-value from 7.3 to 4.0 caused the forisomes to shorten by approximately 15%, while increasing the pH to 11.0 caused them to shorten by 28 to 30%. In both cases, the increases of the forisomes volume were greater than during the Ca^{2+} induced contraction. The pH values of 4.7±0.3, and 10.2±0.2 marked the inflection points of the acid base titration of different forisomes.

Keywords: Chemo-mechanical protein aggregate; Forisome; Contracting behavior; Ca^{2+} induced contraction; pH-induced contraction; Geometric parameters

1. Introduction

Protein based motors [1,2] convert chemical energy directly into mechanical work. During this process, the protein folding state is controlled by chemical reactions, *e.g.* phosphorylation of the hydroxyl groups of serine, hydroxyproline and tyrosine residues, the chelation of Ca^{2+} ions, the protonation of amino and carboxyl groups, and the deprotonation of ammonium and carboxylic acid groups. In addition to nucleoside triphosphate dependent molecular motors [1], other protein-based motors propelled directly by Ca^{2+} ions, *e.g.* spasmonems [2] and forisomes [3–5] and by pH gradients, *e.g.* forisomes [4] and bacterial flagella [6] have been identified.

Forisomes are aggregates of P-proteins found in the phloem cells of legumes (*e.g. Vicia faba*) [7,8]. They undergo conformational change from a longitudinally expanded to a longitudinally contracted state, in response to the addition of Ca^{2+} or pH shifts [4]. *In vivo*, Ca^{2+} induced forisome contraction is a response to osmotic or mechanical stress resulting Ca^{2+} transport through ion channels into the phloem cell as described by Knoblauch et al. [7]. The forisomes also swell strongly as they contract.

Inspired by results described by Knoblauch et al. [4], we set out to analyze the contraction behavior and stability of forisomes in more detail. Specifically, we aimed to carry out a quantitative analysis of their interaction with Ca^{2+} and other bivalent metal ions at different concentrations. We investigated the stability and the changing of their geometric parameters taking into consideration the dependence on dissolved oxygen. To gain a better insight into the pH-dependent contraction of forisomes and to

* Corresponding author. Tel.: +49 345 55 89 123; fax: +49 345 55 89 101.
E-mail address: spn@iwmh.fhg.de (U. Spohn).

0301-4622/$ - see front matter © 2006 Elsevier B.V. All rights reserved.
doi:10.1016/j.bpc.2006.10.008

determine the corresponding points of inflection, we investigated their contraction behavior as a function of pH in the range 2–12.

2. Materials and methods

2.1. Isolation and purification of forisomes

Forisomes were isolated from *Vicia faba* using a procedure modified slightly from that described by Knoblauch et al. [4]. *Vicia faba* plants were grown in pots of sterilized garden mould in a greenhouse with 14-h photoperiod. The plants were irrigated extensively, 6 weeks after germination. The first three internodes (counted from the base of each plant) were then excised, and transferred into Ca^{2+}-free measuring M buffer (0.1 M KCl, 10 mM Tris, pH 7.3) containing 10 mM EDTA. Opposing excisions were made in the rind of the plants, and the rind was peeled away. The phloem tissue was then removed by scratching with a scalpel, and transferred into the buffer described above. The separated phloem tissue was dried with paper tissues, ground under liquid nitrogen, and suspended in a fresh preparation of the buffer. The suspension was then filtrated through a nylon sieve with a mesh size of 55 μm. The filter cake was rinsed several times with small amounts of buffer and stored at −80 °C.

2.2. Measuring apparatus

Fig. 1 shows the measuring and observation cell, which consisted of a measuring chamber (MC) and an inflow (I) for the conditioning and rinsing solutions (S1 and S2), a transfer channel (TC), and the storage chamber (SC) with the outflow (02) for the rinsing solution. The flow and exchange of the conditioning and rinsing solutions S1 and S2 were adjusted by three computer controlled piston pumps (Metrohm Dosimat 665, Herisau, Schwitzerland). To adjust the concentrations of Ca^{2+} and EDTA or the pH two pumps were combined to mix the two conditioning solutions. The solutions were mixed in a knotted tube reactor (MT) with a tube diameter of 0.5 mm (tube length 30 cm) or in a magnetically stirred vessel with a volume

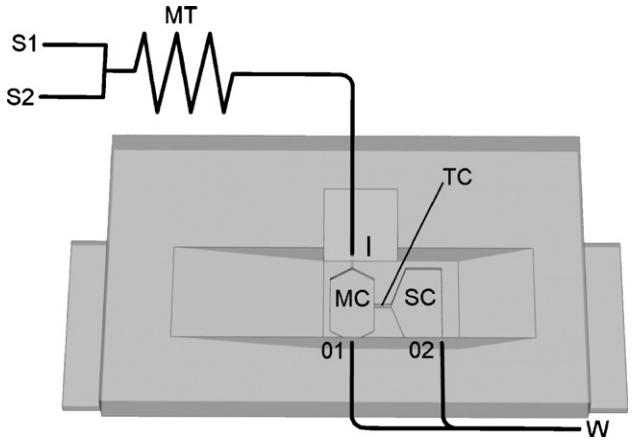

Fig. 1. Design of the measuring cell, MC — measuring chamber, SC — storage chamber, S1 and S2 — measuring solutions, MT — coiled mixing tube, I — inflow, 01 and 02 — outflow, W — waste.

of 5 mL. The pumps and the measuring cell were connected by Teflon tubes with an inner diameter of 0.5 mm. This apparatus had resolutions of 0.5 μL and of 10 $\mu L/min^{-1}$ for the volume and the flow rate, respectively, allowing the concentrations to be adjusted very precisely by varying the flow rate ratio of the piston pumps within the range 1:10 to 10:1. A computer-controlled peristaltic pump (Miniplus 3, Gilson International, Den Haag, The Netherlands) removed the rinsing and waste solutions from the storage and measuring chambers.

The measuring cell was mounted on the table of an Axiovert 25 C microscope (Zeiss, Wetzlar, Germany), which was maintained at 25 °C ± 0.5 K using a thermostate. Sample positioning and repositioning, objective selection and focusing, and the adjustment of the condenser light were automated. A micromanipulator (Luigs and Neumann) with automatic *xyz*-adjustment was used to fix and localize the forisomes in the measuring chamber. In the storage chamber, single forisomes were captured using a thin glass capillary tip and transferred through the narrow channel (TC) into the measuring chamber by exploiting the slight reverse flow of the measuring solution. The micromanipulator included a glass pipette with a long pulled tip (diameter < 2 μm). With the exception of the pumps, the entire set-up was mounted on an actively damped optical bench (I-325A, Newport, Darmstadt, Germany). A video camera (JVC TK-C1481BEG, JVC, Japan) was installed at the appropriate microscope port and connected to a PC by a frame grabber card (HaSoTec GmbH, Rostock, Germany). A software package was developed to allow automatic control the microscope, the piston pumps and the image [9].

For imaging by scanning electron microscopy (SEM), the forisomes were isolated by Nycodenz^R-density-gradient centrifugation, freeze-dried as described previously [4], and resuspended in M buffer. Droplets of the suspension were transferred to custom-made patches of nanoporous Al_2O_3 membranes [10] or microporous polycarbonate membranes, on which the forisomes were allowed to settle. Some batches were incubated in 10 mM $CaCl_2$, 0.1 M Tris (pH 7.3) to study longitudinally contracted forisomes. The forisomes were initially fixed in PBS buffer (4.3 mM Na_2HPO_4, 1.4 mM KH_2PO_4, 137 mM NaCl, 12.7 mM KCl, pH 7.5) containing 2.5% of glutaraldehyde, and then washed three times in PBS for 5 min and post-fixed in 2% OsO_4 in PBS for 2 h. The OsO_4 solution was replaced with distilled water. Dehydration was accomplished by a series of aqueous solution of acetone (25%, 50%, 70%, 90%, 95%, and 100%; 30 min each). In a final step, the samples were dried in a critical point dryer (CPD 030, Bal-Tec, Balzers, Liechtenstein) with liquid CO_2. The Al_2O_2 membrane patches were fixed on holders and sputtered with platinum (sputter-coater B30, VEB Hochvakuumtechnik, Dresden, Germany). The patches were inspected using a cold field emission SEM (S4500, Hitachi, Tokyo, Japan) at accelerating voltages of 1–10 kV.

2.3. Measurement of changing geometric parameters

To measure the geometric parameters of individual forisomes *in situ*, the tips of purified forisomes were allowed to adhere to the glass surface of a micropipette tip (diameter < 2 μm), and the

forisomes were aligned by the flowing field of the conditioning solution before the flow was stopped, and the image processing was initiated. The length and diameter of the forisomes were determined using the program Analysis (SIS Soft Imaging System GmbH, Münster, Germany) to evaluate the recorded video images.

In the first series of experiments, the Ca^{2+} concentration was alternated between 0 and a particular upper value to induce forisomes to change between the longitudinally expanded and the contracted states. In the second set of experiments, the concentration of free Ca^{2+} was varied continuously varied by titration with EDTA in a stirred vessel. EDTA forms at pH 7.3 the Ca-EDTA complex with a conditional stability constant of $\log K_{SCaEDTA} = 7.72$ in comparison to the stability constant of the Ca-EGTA complex: $\log K_S = 7{,}13$. The Ca^{2+} concentration was recorded continuously using a Ca^{2+}-sensitive electrode (WTW, Weilheim Germany). In analogous *in vitro* experiments, the Ca^{2+} was replaced with Sr^{2+}, or Ba^{2+}. The influence of pH on contraction was investigated in a 50 mM glycine, 50 mM NaCl buffer to which 50 mM HCl or 50 mM NaOH was added to adjust the pH to values between 2.0 and 3.4, and between 9.0 and 12.3, respectively. Within the pH range 3.4–6.0, the buffer was 100 mM sodium actetate adjusted with acetic acid or 0.1 M NaOH. Within the pH range 6.5–9.0, the buffer was 50 mM Tris buffer adjusted with 1 M HCl.

3. Results and discussion

3.1. The dependence of the Ca^{2+}-induced contraction on dissolved oxygen

Initial experiments showed that the forisomes are inactivated slowly. The repeated contraction of several forisomes was seen to decrease slowly with time, and reached approximately 10% of the initial value after 8 h of periodic changing the Ca^{2+} concentration. We therefore, investigated the forisomes contraction both in an air-saturated medium and in a medium containing 10 mM hydrogen sulfite and Co^{2+} to remove dissolved oxygen. The concentration of the dissolved oxygen was measured using a CLARK oxygen electrode, and none could be detected after 1 min after the addition of 10 mM hydrogen sulfite and 5 μM $Co(NO_3)_2$ to the M-medium. In the presence of 2–5 μM of Co^{2+} ions, this high concentration of hydrogen sulfite concentration can compensate for the back-diffusion of oxygen from the atmosphere into the measuring chamber. Fig. 2a and b show the changes of normalized forisomes lengths measured in the air-saturated and in the oxygen-free media, respectively. In the air-saturated medium, the time between the contraction step (initiated by the addition of 10 mM Ca^{2+}) and the stretching step (initiated by the addition of 10 mM EDTA) was adjusted to 10 min. The forisome was strongly inactivated in the presence of dissolved oxygen after just 10 min in the contracted state. The change of the normalized length decreased to less than 30% of its initial value. This result appears to contradict data published by Knoblauch et al. [4], but these investigators described fast experiments of forisomes contraction lasting only seconds in oxygen containing aqueous solutions. In the longitudinally expanded state the forisome remained active for at least 2 h also in air saturated M-medium. Under anaerobic conditions, the forisome conversion cycles remained more stable, maintaining their amplitude of contraction for about 80 min (Fig. 2b). These experiments were repeated three times with three different forisomes.

When the forisome were exposed to Ca^{2+} for less than 20 s and then induced to change back by the EDTA in the M buffer, the amplitude of contraction remained almost stable in the air-saturated M-medium. We conclude that forisome inactivation by dissolved oxygen occurs more readily in the contracted state compared to the expanded state. However, contracted forisomes did not change in length or diameter after more than 4 h in the presence of dissolved oxygen.

Neither 5 μM Co^{2+} nor 10 mM HSO_3^- had a significant impact on the contraction process. Since 5 μM Co^{2+} cannot induce the contraction of expanded forisomes and does not influence Ca^{2+}-dependent contraction at Ca^{2+} concentrations higher than 0.5 mM, competition between Ca^{2+} and Co^{2+} ions for hypothetical binding sites in the forisomes do not play a significant role under these conditions.

Our investigations showed that the contraction and cycling process cannot be fully reversed in the presence of dissolved oxygen. We propose that dissolved oxygen also causes conformational changes in the protein molecules of the

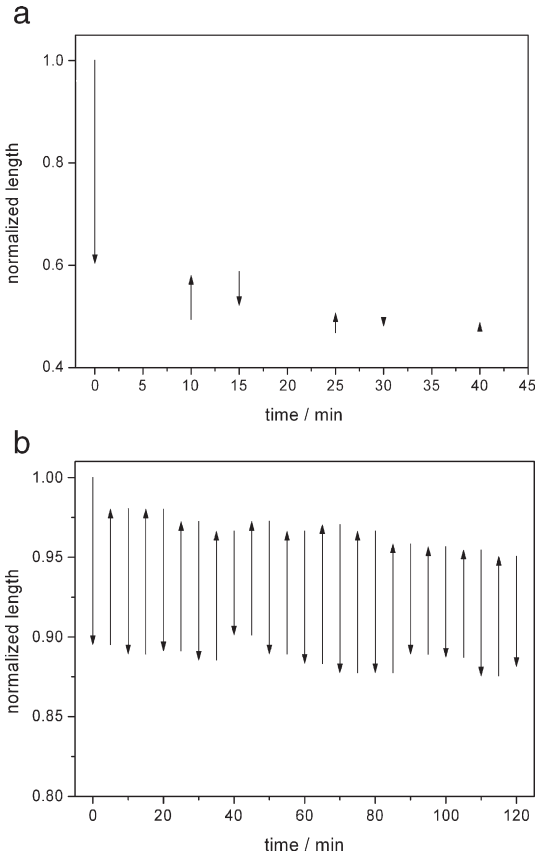

Fig. 2. The stability of the amplitude of contraction when cycled between 10 mM EDTA and 10 mM Ca^{2+} measured for a fixed forisome in a) air-saturated and b) in oxygen free M buffer additionally containing 5 mM $NaHSO_3$ and 5 μM $CoCl_2$.

forisome by oxidizing free mercapto groups and forming disulfide bridges between the cysteine molecules in a section of the protein sequence identified by Noll [12]. It was demonstrated in many experiments that the contracted forisomes are more rapidly and stronger destabilized than longitudinally expanded forisomes.

3.2. Geometric parameters in the final states of conversion

We set out to determine the geometric parameters of forisomes and their statistical distribution, in order to investigate their mechanical behavior and to be able to estimate the achievable conversion of chemical free energy into mechanical work with respect to the forisome volume in a later research work. The Fig. 3a and b show the same forisome fixed on the tip of a glass capillary in, respectively, their longitudinally expanded and in the contracted state. In the expanded state, the forisome appears to consist of bundles as shown in the SEM image (Fig. 4a). In the contracted forisome, the fibrous bundles adhere to form a body as shown in the corresponding SEM image (Fig. 4b). The forisomes consist of smaller protein aggregates, which can be observed as structured subunits of the protein aggregates, also in this conversion state.

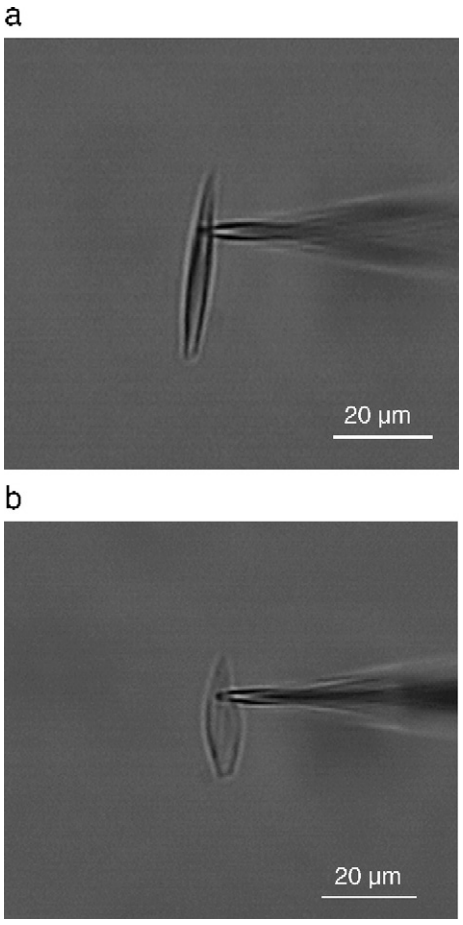

Fig. 3. a — A forisome in the longitudinally expanded state in the M-buffer containing 10 mM EDTA; b — a forisome in the final contracted state in the M-buffer containing 10 mM Ca^{2+}.

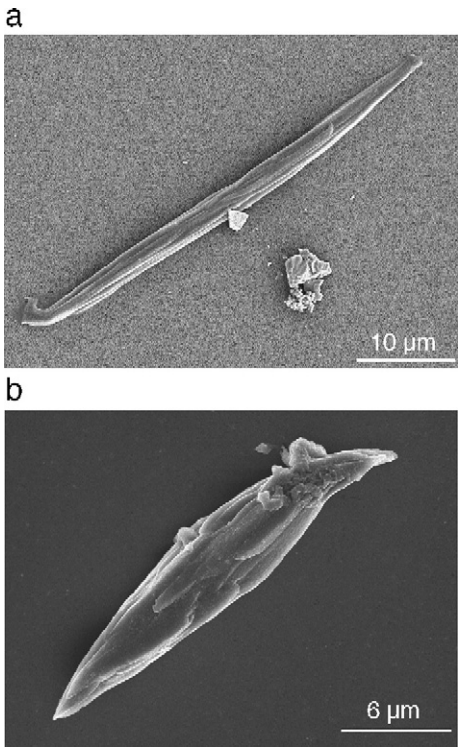

Fig. 4. a — Longitudinally expanded forisome, exposed to Ca^{2+}-free medium, b — contracted forisome, in M buffer containaining 10 mM of free Ca^{2+} ions, SEM images recorded at 6 KV.

The contracted forisome with a length of 24 µm and diameter of 5.1 µm is much shorter and thicker than the longitudinally expanded forisome with a length of 47.2 µm and a diameter of 2.8 µm resulting in a volume ratio of 1.65. Therefore, it can be assumed that the contracted forisome has a lower density. Since both forisomes were prepared and imaged under high vacuum ($<10^{-5}$ Torr) we can assume that at least a proportion of the uptaken water is tightly bound also within the contracted forisome, since loosely bound water would be lost by evaporation.

Fig. 5 shows the distributions of the optically measured aspect ratios of 318 expanded and 111 contracted forisomes.

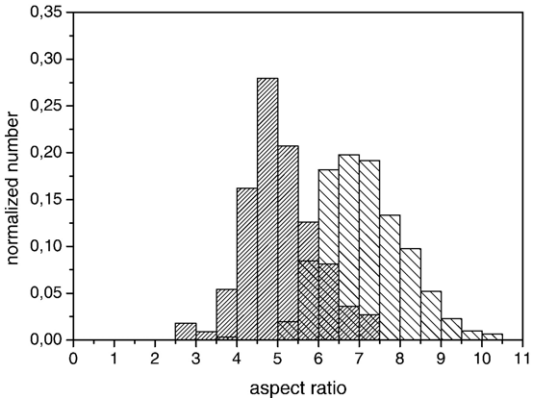

Fig. 5. Distribution of the aspect ratios for 318 longitudinally expanded forisomes (wider hatched bars) in M buffer containing 10 mM EDTA solution, and of 111 contracted forisomes in M buffer containing 10 mM Ca^{2+}.

Table 1
Geometric parameters of forisomes (another charge of forisomes as investigated for the size distributions shown in Fig. 4) in the corresponding states measured during different contraction experiments (confidence intervals with $n=13$ for the contraction processes 1. and 2., and $n=49$ for contraction processes 3., $\alpha=0.05$)

Mean lengths in µm			
contraction process	$l_{expanded}$	$l_{contracted}$	$\Delta L=(l_{contracted}-l_{expanded})/l_{expanded}$
1. pH 7.3 → pH 4.5	32.0±2,3	24.7±2,6	−0.23±0,05
2. pH 7.3 → pH 11.0	38.4±2.8	31.8±4.0	−0.17±0.05
3. [Ca^{2+}] 0 → 10 mM	38.1±1.6	31.0±1.7	−0.18±0.03
Mean diameters in µm			
	$d_{expanded}$	$d_{contracted}$	$\Delta D=(d_{contracted}-d_{expanded})/d_{expanded}$
1. pH 7.3 → pH 4.5	4.4±0.4	8.4±1.0	0.91±0.20
2. pH 7.3 → pH 11.0	4.9±0.3	12.3±1.6	1.51±0.30
3. [Ca^{2+}] 0 → 10 mM	4.7±0.2	8.5±0.5	0.81±0.09
Aspect ratio			
	$a_{stretched}$	$a_{contracted}$	Δa
1. pH 7.3 → pH 4.5	7.3±1.0	2.9±1.1	−4.4±1.5
2. pH 7.3 → pH 11.0	7.8±1.3	2.6±1.4	−5.3±1.9
3. [Ca^{2+}] 0 → 10 mM	8.1±0.8	3.7±0.7	−7.1±1.0
Mean volumes in fL			
	$v_{expanded}$	$v_{contracted}$	$\Delta v=(v_{contracted}-v_{expanded})/v_{expanded}$
1. pH 7.3 → pH 4.5	335±67	982±206	1.93±0.60
2. pH 7.3 → pH 11.0	506±85	2478±470	3.90±1.10
3. [Ca^{2+}] 0 → 10 mM	464±45	1048±155	1.26±0.20

When 10 mM of Ca^{2+} ions were added to the solution of conversion, the forisomes contracted and swelled to 2–3 times their initial volume. Because the converting times were smaller than 10 s dissolved oxygen had no influence on the measurement of the geometric parameters.

We propose a thermodynamic cycling process to explain forisome behavior, as shown in Fig. 6. This process involves a reversible transformation between the expanded and contracted states. The reaction between Ca^{2+} and EDTA is the resulting reaction and provides the free reaction energy for this cycle process. The highly stable molecule CaH_2EDTA is formed by the chelation of Ca^{2+} by EDTA, a reaction with a Gibbs free energy of $\Delta_R G=-43.3$ kJ mol^{-1}, calculated from the conditional stability constant $K=5.24\times10^7$ L mol^{-1} of the complex at pH 7.3 and $T=20$ °C. When cycling process begins, the forisome binds Ca^{2+}, which induces a conformational change. Simultaneously, the forisome takes up a large amount of water, which causes it to contract longitudinally and swell laterally. The light microscope and SEM images (Figs. 3b and 4b) indicate that water is highly ordered in the contracted state, which would result in a significant decrease in entropy. Assuming that forisomes normally have rotationally symmetrical ellipsoid shape, the averaged volume increases from (464±45) fL to (1048±155) fL (see also Table 1). Given the density of water is 1 kg L^{-1}, we estimate that approximately 2×10^{13} water molecules are taken up per forisome. Forisome contraction appears similar to the conformational change that occurs in aggregates of elastin-like proteins, when they reach the so-called inversion temperature T_i [11]. This same process can be induced at lower temperatures in certain chemical environments, *e.g.* by dephosphorylation of phosphatidyl groups and by changing the pH to neutralize either ammonium or carboxylate groups. In forisomes, we thus assume that the complexation of the Ca^{2+} ions by carboxylate and amino groups induces a change of the folding state of the assembled protein molecules. However, the mechanistic basis of forisome contraction following the uptake of water remains to be explained. The addition of EDTA to the forisomes caused bound Ca^{2+} ions to be eliminated from the corresponding protein molecules, and induces a change back to the original, longitudinally extended conformation, accompanied by the expulsion of a great number of water molecules increasing the entropy (Fig. 6). In this unloaded cycle process the free reaction energy is completely dissipated into thermal energy. The investigation of the loaded cycle process, *e.g.* during the bending of thin glass fibers will be described elsewhere.

Another Ca^{2+}-sensitive protein aggregate, the spasmoneme from *Vorticella* sp. is known to behave in a similar manner [13,14]. This structure contracts strongly following exposure to Ca^{2+} and swells when the Ca^{2+} ions are sequestered by a chelating agent such as EGTA. However, there appears to be no obvious homology between the forisome P-protein [12] and the known spasmin proteins which form spasmoneme [15]. There also appears to be no homology between forisomes proteins and other EF-hand Ca^{2+} binding proteins such calmodulin and troponin C.

As demonstrated previously by Knoblauch et al. [4], forisomes also respond to pH changes in the acid pH range pH 4.9–4.5 and at alkaline pH values greater than 9.6. Table 1 shows how the geometric parameters of forisomes are affected by pH changes in the ranges 7.3–4.5 and 7.3–11.0, compared to the changes induced by 10 mM Ca^{2+}. In both pH ranges, the change in forisome length is similar to that induced by 10 mM Ca^{2+} and 10 mM EDTA. However, the changing from pH 7.3 to 11 approximately doubles the diameter of the forisomes. The

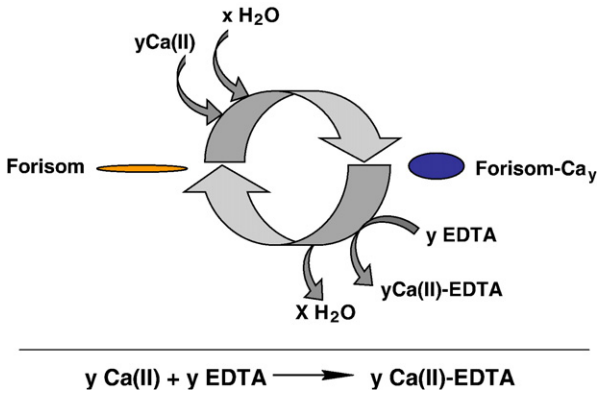

Fig. 6. Scheme of the thermodynamic cycle of contraction propelled by the complexing reaction between Ca^{2+} and EDTA. The variables x and y refer to the number of water molecules and Ca^{2+} ions, respectively.

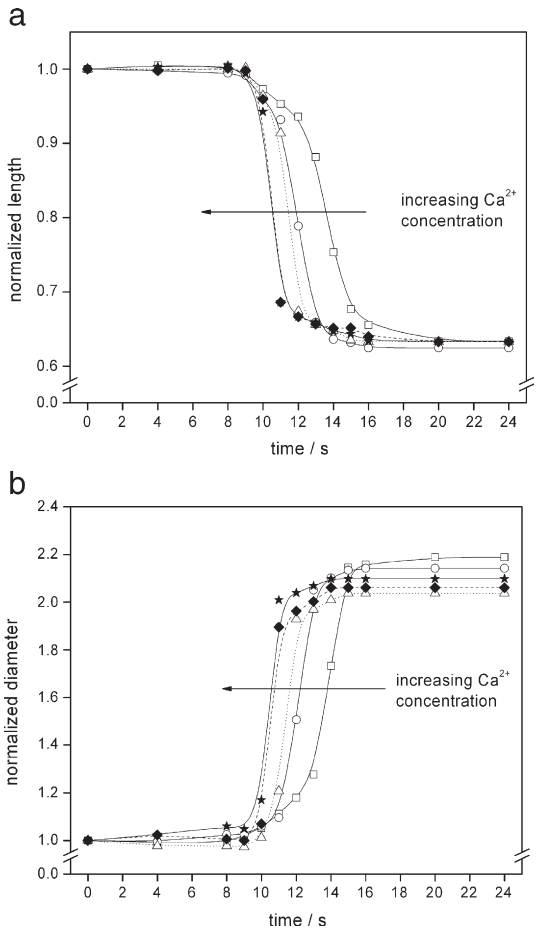

Fig. 7. Dependence of a — the normalized forisome length and b — the normalized diameter on the measuring time after changing over from 10 mM EDTA to different concentrations of Ca^{2+} in the M buffer, −□− 200 μM, −○− 400 μM, −Δ− 600 μM, −◆− 800 μM, −★− 1000 μM.

forisomes consists almost entirely of proteins. Therefore, we suggest that changes the pH from 7.3 to 4.5 causes the partial protonation of side chain carboxylate groups of aspartic acid (pK_a=3,90) and glutamic acid (pK_a=4.07), and the higher degree of protonation of the imidazoyl group (pK_a=6.04) of histidine as earlier proposed and taking into consideration the

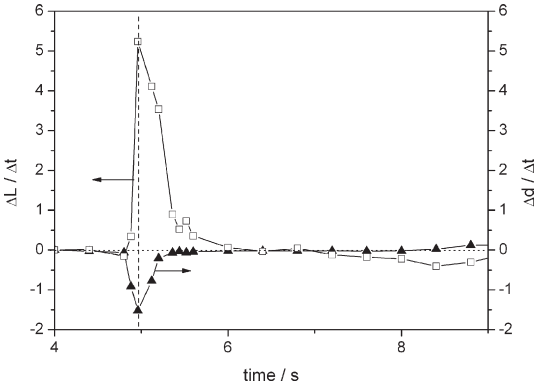

Fig. 8. The change of forisome length ($\Delta L/\Delta t$ in μm/s) and forisome diameter ($\Delta d/\Delta t$ in μm/s) depend on the time taken to change over from 1 mM EDTA to 1 mM Ca^{2+} in the M-buffer, pH 7.3.

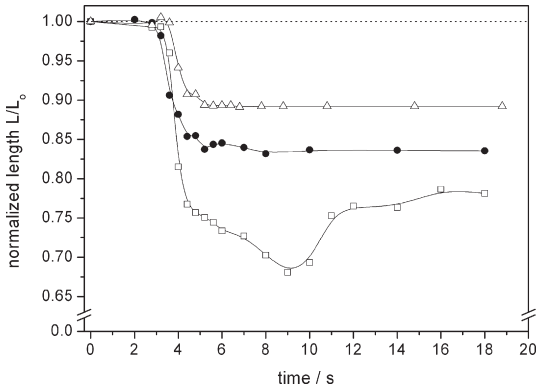

Fig. 9. Dependency of the relative forisome length on measuring time after changing over from the M buffer containing −△− 10 mM Ba^{2+}, −●− 10 mM Sr^{2+}, −□− 10 mM Ca^{2+}, L_o=36.8 μm.

paper of Pickard et al. [16]. Furthermore, we propose that ε-ammonium groups of lysine and hydroxyl groups of tyrosine are deprotonated as the pH increases from 7.3 to 11.0 at least partly. These considerations are based on the assumption that the forisome proteins contain these amino acids and the shift of their pK_a values is not significantly influenced by intramolecular interactions.

It is possible that the incorporation of water in forisomes is analogous to the hydration of hydrophobic side chains of elastin-like proteins when its inverse transition temperature is shifted to values higher than the ambient temperature, as described by Urry et al. [17–19]. We assume that protonation of carboxylate groups and/or imidazoyl groups or deprotonation of ε-ammonium groups can induce the corresponding change of protein conformation into a state able to bind water around hydrophobic side chains. However, without detailed informations about the sequence of the chemomechanically active forisome protein and their 3D structure, any assumption about the molecular mechanism of forisome contraction remains a speculation.

As shown in Table 1, an alkaline pH-shift leads to an increase in forisome volume that is more than double that induced by an

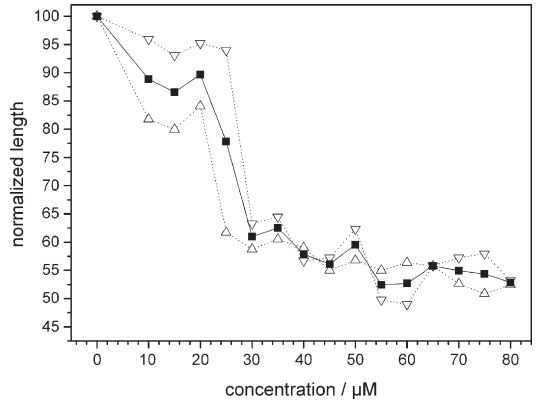

Fig. 10. Averaged titration course resulting from two titrations of a fixed forisome performed in the presence of 10 mM citrate by the incremental addition of 10 mM Ca^{2+} solution to a mixing vessel filled with M-buffer at pH 7.3 just before pumping the resulting solution through the measuring chamber.

acid pH shift, but in both cases the increase in volume is from 1.5 to three times greater than can be achieved using Ca^{2+}.

3.3. Ca^{2+}-titration of single forisomes

To obtain more precise quantitative data about Ca^{2+} dependent contraction behavior, forisomes were contacted consecutively with different Ca^{2+} concentrations. The Ca^{2+} concentrations were measured potentiometrically by using the Ca^{2+}-ISE calibrated in the range between 1 μmol L^{-1} and 10 mM Ca^{2+} in M-medium at the measuring conditions. In the absence of any chelator, the blank concentration of Ca^{2+} was between 1 and 2 μmol L^{-1} in the M-medium. Fig. 7a and b show that the relative length and normalized diameter of a forisome is dependent on the measuring time for changing between 10 mM EDTA in the M-buffer to the appropriate Ca^{2+} concentration. The measuring data were calculated from a video film sequence by evaluating one image per second. Where the [Ca^{2+}]-concentration fell within the range 200– 1000 μM, there was no significant difference between the final geometric parameters. However, the conversion time decreased by 3 to 3.5 s, reflecting the shorter time taken to reach the equivalence point between EDTA and Ca^{2+} with increasing Ca^{2+} concentrations. Stationary concentrations are achieved in the measuring chamber after 10–12 s. This was shown in tracer experiments in which the conductivity at the outlet was measured after stepping up the KCl concentration at the inlet from 0 to 1 M. The conversion times are much shorter than the time taken to achieve the final Ca^{2+} concentration and cannot be resolved precisely. Conversion times of <0.1 s can probably be achieved in fixed forisomes given the steep increase in Ca^{2+} concentration occurring after the very fast injection of 1 mL 10 mM Ca^{2+} by pipette into the buffering solution containing 0.1 mM EDTA.

As shown in Fig. 8 the diameter and length of the forisoms change almost synchronously following the addition of 1 mM Ca^{2+}, the change in length lagging very slightly behind. Taking the time resolution of the measuring apparatus into account, we conclude that the longitudinal contraction and lateral swelling of the protein aggregate occur almost simultaneously.

Contracted forisomes change back to the longitudinally expanded conformation, when the 10 mM Ca^{2+} solution is replaced with solutions containing 10 mM citrate, 10 mM ATP or 10 mM EDTA in the aqueous primary buffer adjusted to pH 7.3. Contracted forisomes also change back when incubated in double-distilled water for at least 10 min. The back-converting time increases in the order EDTA (<1 s)<citrate<ATP<H_2O showing that the process is influenced by the Ca^{2+} binding constants of these chelators.

Fig. 9 shows the time-dependent change in the normalized length L/L_o of a forisome in 10 mM Sr^{2+} and 10 mM Ba^{2+}, compared to 10 mM Ca^{2+} in the M buffer. L_o is the initial length of the forisome and L is the length after contraction. The change in length seems to depend on the type of metal ion, suggesting that the ion radius influences binding strength and thus the

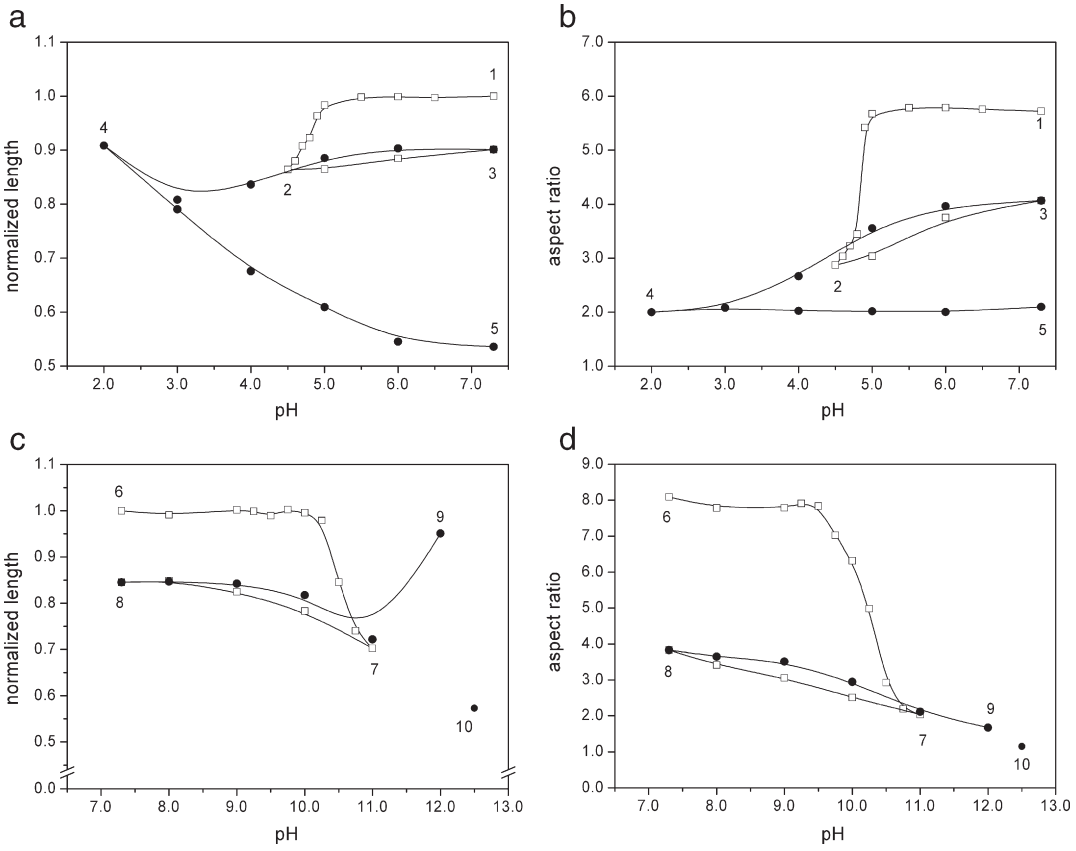

Fig. 11. The geometric parameters of forisomes change as a function of pH. All buffer solutions contained 0.1 M KCl and 10 mM EDTA, –□– with decreasing pH; –●– with increasing pH.

resulting conformational change in the forisome. The effective influence of the earth alkaline ions will be reinvestigated in the absence of dissolved oxygen and any other doubly charged metal ion in a later work. When immersed in 10 mM Ca^{2+} the forisome initially contracts rapidly, and then relaxes more slowly to achieve its final normalized length value, which is significantly lower than can be achieved in the presence of the other metal ions. During Sr^{2+}- and Ba^{2+}-induced change of state, the final state is reached without characteristic over-contraction and relaxation seen with Ca^{2+}. However, the first derivatives of the courses of conversion achieve their maxima at approximately the same time.

Two forisomes were titrated with a series of *in situ* prepared Ca^{2+} solutions in the absence of dissolved oxygen. Fig. 10 shows a curve averaged from two titrations recorded for two forisomes from the same charge. The inflection point was identified as (25±3) μM Ca^{2+}. Knoblauch et al. [4,5] published a corrected threshold value of 60–90 μM Ca^{2+} for the same kind of forisomes based on basic contraction experiments, proposing an "all-or-non-mechanism" to explain the results. Our titration experiments demonstrated clearly that forisome length, and probably also the other geometric parameters are a function of the Ca^{2+} concentration. The geometric parameters of the forisomes are changing continuously through infinitesimal states.

An averaged dissociation constant K_m of (22±3) μM can be calculated, based on the dependence of forisome contraction on Ca^{2+} concentration. This can be shown using a Hill plot based on Eq. (1), where n is the number of Ca^{2+}-binding sites in the contracting protein molecules. L^* is defined by Eq. (2), where L_{min} and L_{max} represent forisome length in the completely contracted and expanded states, respectively. An averaged n-value of 2.2 was calculated from the titration of 13 individual forisomes [19].

$$\lg((1-L^*)/L^*) = n \cdot \lg[Ca^{2+}] - n\lg K_m \quad (1)$$

$$L^* = (L-L_{min})/(L_{max}-L_{min}) \quad (2)$$

Asai et al. [20,21] proposed a similar model for the contraction of spasmonemes, which like forisomes are relatively large protein aggregates with a similar size. These show longitudinal contraction when the Ca^{2+} concentration increases above a threshold value of 1 μM.

The back-titration of contracted and swollen forisomes with 10 mM citrate under the same conditions revealed a significant hysteresis. This primarily reflects the fact that forisomes have different response times to Ca^{2+} and citrate in the Ca^{2+} loaded state.

3.4. Influence of pH on the geometric parameters of the forisomes

We initially recorded forisome behavior in buffers with pH values ranging between 7.3 and 2.0. Fig. 11a and b show that the relative length and the aspect ratio of forisoms is dependent on the pH. Measuring points 1–5 correspond to the pictures 1–5 in Fig. 12. By decreasing the pH value stepwise from 7.3 to 4.5, a typical titration curve was recorded with an inflection point of pH=(4.7±0.3). This agrees with data previously published by Knoblauch et al. [4], who stated that when the pH is gradually reduced, forisome contraction occurs suddenly at pH 4.9. In our experiments, the length of the forisome reduced from 31.2 to 26.9 μm concomitant with significant lateral swelling. When the pH was gradually increased, the forisome expanded but did not return to its initial length. The final length was 28.1 μm at pH 7.3. The reduced stability of the forisome proteins at non-physiological pH values and in the presence of dissolved oxygen is likely to be responsible for this irreversible deactivation of the forisomes. Further investigations are necessary to distinguish between these different influences.

When the buffer was acidified again, the same forisome showed only a small reduction in length but a much more significant change in diameter and aspect ratio, with noticeable swelling. However, the protein aggregates remained structured even at pH values as low as 2.0. Bringing the pH back to pH 7.3 in steps of 1 pH unit resulted in surprisingly strong and isotropic shrinking of the forisome, as shown in Fig. 12 part 5. Complete denaturation occurred at pH values <2. However, the forisome could be converted several times between pH 2 and pH 7

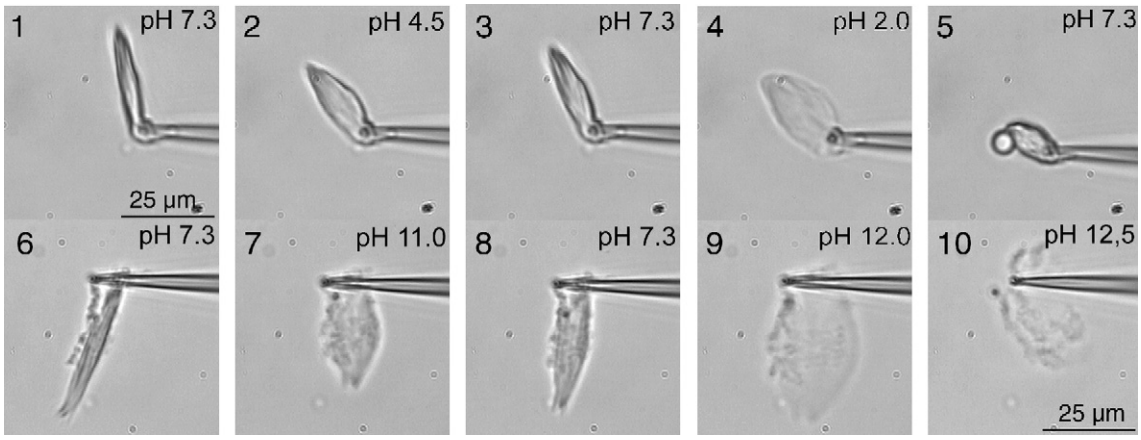

Fig. 12. Forisome structures imaged by optical microscopy at sequentially adjusted pH-values.

without a significant change in aspect ratio, although changes in volume were apparent.

The Fig. 11c and d show the behavior of contraction in the pH range 7.3–12.5. Measuring points 6–10 correspond to the pictures 6–10 in Fig. 12. By increasing the pH value stepwise from 7.3 to 11.0, a typical titration curve was recorded with an inflection point at pH = (10.3 ± 0.2). The forisome contracted by almost 30% with respect to its initial length and swelled strongly. The diameter (data not shown) increased by a factor of at least 2.7. However, this titration of contraction is not reversible. During the stepwise backshift from pH 11 to 7.3, the forisome returned to only 84–85% of the initial length. The second, stepwise pH shift into the alkaline pH range resulted in a relatively small contraction without noticeable change in aspect ratio. The contraction curve resembles the change back curve recorded immediately before, with very pronounced swelling but minimal longitudinal contraction when the pH was increased to 12.0. However, the forisome diameter increased by a factor of at least four. At pH values higher than 11, the forisome expanded isotropically and appeared to be held together by a system of protein fibers. The volume increased by a factor of 4.0–4.5 up to pH 12.0 and remains of the fibrous structure could be seen. All forisome structure was destroyed at pH 12.5.

The rapid changing of the forisomes length between neutral and acid conditions (pH 7.3 and 4.5), and between neutral and alkaline conditions (pH 7.3 and 11), was repeatable, but only with a significant loss of amplitude. In the neutral-acid cycle, the amplitude fell continuously from second cycle, to a final value of 32–33% relative to the initial amplitude by the 15th cycle. In the neutral alkaline cycle, the final value was 50–52% of the initial amplitude. The initial amplitude of contraction was 17% of the initial forisome length in the neutral-acid cycle, and 32–33% of the initial forisome length in the neutral-alkaline cycle.

Acknowledgement

The authors would like to thank M. Knoblauch, W. Peters, D. Prüfer and G. Noll for helpful discussions. This work was supported by an internal research program of the Fraunhofer Gesellschaft.

References

[1] J. Howard, Mechanics of Motor Proteins and the Cytoskeleton, Sinauer Associates Inc, Sunderland, MA, 2001.

[2] W.B. Amos, Molecules and cell movement, in: S. Inoue, R.E. Stephens (Eds.), Contraction and Calcium Binding in the Vorticellid Ciliates, Raven Press, New York, 1975, pp. 411–435.

[3] M. Knoblauch, W.S. Peters, Forisomes, a novel type of Ca^{2+}-dependent contractile motor, Cell Motil. Cytoskelet. 58 (2004) 137–142.

[4] M. Knoblauch, G.A. Noll, T. Müller, D. Prüfer, I. Schneider-Hüther, D. Scharner, A.J.E. van Bel, W.S. Peters, ATP-independent contractile proteins from plants, Nat. Mater. 2 (2003) 600–603.

[5] M. Knoblauch, G.A. Noll, T. Müller, D. Prüfer, I. Schneider-Hüther, D. Scharner, A.J.E. van Bel, W.S. Peters, Corrigendum, Nat. Mater. 4 (2005) 353.

[6] S. Kojima, D.F. Blair, The bacterial flagellar motor: structure and function of a complex molecular machine, Int. Rev. Cyt. 233 (2004) 93–134.

[7] M. Knoblauch, W.S. Peters, Reversible calcium-regulated stopcocks in legume sieve tubes, Plant Cell 13 (2004) 1221–1230.

[8] K. Ehlers, M. Knoblauch, A.J.E. Van Bel, Ultrastructural features of well-preserved and injured sieve elements: minute clamps keep the phloem transport conduits free for mass flow, Protoplasma 214 (2000) 80–92.

[9] Ch. Francke, Diploma Thesis, University of Applied Sciences, Merseburg, 2004.

[10] A. Heilmann, N. Teuscher, A. Kiesow, D. Janasek, U. Spohn, Nanoporous aluminum oxide as a novel support material for enzyme biosensors, J. Nanosci. Nanotechnol. 3 (2003) 1–5.

[11] D.W. Urry, Physical chemistry of biological free energy transduction as demonstrated by elastic protein-based polymers, J. Phys. Chem. 101 (1997) 11007–11028.

[12] G. Noll, Thesis of doctoral dissertation, University of Gießen, 2006.

[13] Y. Moriyama, S. Hiyama, H. Asai, High-speed video cinematographic demonstration of stalk and zooid contraction of *Vorticella convallaria*, Biophys. J. 74 (1998) 487–491.

[14] Y. Moriyama, H. Okamoto, H. Asai, Rubber-like elasticity and volume changes in the isolated spasmoneme of giant *Zoothamnium* sp. under Ca^{2+}-induced contraction, Biophys. J. 76 (1999) 993–1000.

[15] J.J. Maciejewski, E.J. Vacchiano, S.M. McCutcheon, H.E. Buhse Jr., Cloning and expression of a cDNA encoding a Vorticella convallaria spasmin: an EF hand calcium-binding protein, J. Eukaryot. Microbiol. 46 (1999) 165–173.

[16] W.F. Pickard, M. Knoblauch, W.S. Peters, A.Q. Shen, Prospective energy densities in the forisome, a new smart material, Mater. Sci. Eng., C, Biomim. Mater., Sens. Syst. 26 (2006) 104–112.

[17] D.W. Urry, Five Axioms for the functional design of peptide-based polymers as molecular machines and materials: principle for macromolecular assemblies, Biopolymers 47 (1998) 167–178.

[18] D.W. Urry, S. Quing Peng, T.A. Parker, Hydrophobicity-induced pK shifts in elastin protein-based polymers, Biopolymers 32 (1992) 373–379.

[19] D.W. Urry, B. Haynes, H. Zhang, R.D. Harris, K.U. Prasad, Mechanochemical coupling in synthetic polypeptides by modulation of an inverse temperature transition, Proc. Natl. Acad. Sci. U. S. A. 85 (1988) 3407–3411.
M. Fritzsche, Physikochemische Untersuchungen zum Schaltverhalten und zur chemomechanischen Kraftwirkung von Forisomen. Master Thesis, University of Halle — Wittenberg, 2005.

[20] H. Asai, T. Ochiai, K. Fukui, M. Watanabe, F. Kano, Improved preparation and cooperative contraction of glycerinated *Vorticella*, J. Biochem. 83 (1978) 795–798.

[21] Y. Yokohama, H. Asai, Contractility of the spasmoneme in glycerinated *Vorticella s*talk induced by various divalent metal and lanthanide ions, Cell Motil. Cytoskelet. 7 (1987) 39–45.